Signaling mechanisms involved in altered function of macrophages from diet-induced obese mice affect immune responses

Qingde Zhou[a], Susan E. Leeman[b,1], and Salomon Amar[a,1]

[a]Department of Periodontology and Oral Biology, School of Dental Medicine; and [b]Department of Pharmacology, School of Medicine, Boston University, Boston, MA 02118

Contributed by Susan E. Leeman, April 29, 2009 (sent for review April 3, 2009)

Recent research links diet-induced obesity (DIO) with impaired immunity, although the underlying mechanisms remain unclear. We find that the induction of inducible NO synthase (iNOS) and cytokines is suppressed in mice with DIO and in bone marrow macrophages (BMMΦ) from mice with DIO exposed to an oral pathogen, *Porphyromonas gingivalis*. BMMΦ from lean mice pretreated with free fatty acids (FFAs) and exposed to *P. gingivalis* also exhibit a diminished induction of iNOS and cytokines. BMMΦ from lean and obese mice exposed to *P. gingivalis* and analyzed by a phosphorylation protein array show a reduction of Akt only in BMMΦ from mice with DIO. This reduction is responsible for diminished NF-κB activation and diminished induction of iNOS and cytokines. We next observed that Toll-like receptor 2 (TLR2) is suppressed in BMMΦ from DIO mice whereas carboxy-terminal modulator protein (CTMP), a known suppressor of Akt phosphorylation, is elevated. This elevation stems from defective TLR2 signaling. In BMMΦ from lean mice, both FFAs and TNF-α—via separate pathways—induce an increase in CMTP. However, in BMMΦ from DIO mice, TLR2 can no longer inhibit the TNF-α-induced increase in CTMP caused by *P. gingivalis* challenge. This defect can then be restored by transfecting WT TLR2 into BMMΦ from DIO mice. Thus, feeding mice a high-fat diet over time elevates the CTMP intracellular pool, initially via FFAs activating TLR2 and later when the defective TLR2 is unable to inhibit TNF-α-induced CTMP. These findings unveil a link between obesity and innate immunity.

Akt phosphorylation | CTMP | innate immunity | iNOS | TLR2

Obesity has been found to lead to diminished immune response. Several epidemiological studies of obese individuals found evidence of increased susceptibility to infections, including postoperative infectious complications (1), and a positive correlation between body weight index and the incidence of nosocomial infections (2). Diet-induced obesity (DIO) interferes with the ability of the immune system to appropriately respond to *Porphyromonas gingivalis* infection (3) and causes a higher mortality rate in mice following infection with influenza virus (4).

Obesity is known to elevate TNF-α levels in the plasma of obese subjects (5, 6). However, macrophage functions are impaired in obese animals, with reduced phagocytic capacity and a defective oxidative burst (7, 8). The reduced cytokine expression in response to infection observed in obese mice has been linked to a dysfunction in macrophages and/or a defect in maturation of monocytes (3, 4, 9). Moreover, the ability of mature macrophages from an obese individual to elicit an antimicrobial and cytotoxic response may be inhibited (10). Macrophages sense the presence of microorganisms via pattern recognition receptors, especially members of the Toll-like receptor (TLR) family, and subsequently activate proinflammatory signal pathways. TLR2 is an important receptor by which macrophages recognize *P. gingivalis* (11–14), and mediates destructive chronic inflammatory reactions or confers host protection against *P. gingivalis* in acute infections (12). In addition, TLR2 can be activated by palmitate, a nutritional free fatty acid (FFA), leading to the induction of inflammation and insulin resistance (15). Therefore, the decreased immune responses observed in obese individuals may be related to the disruption of TLR2 signaling pathway by elevated plasma FFAs or by a DIO-related state of chronic inflammation.

One of the fastest and most effective defense mechanisms for macrophage response to bacterial infections is the production of the free radical NO (16–18), mediated by the regulated expression of inducible NO synthase (iNOS) (19). This enzyme catalyzes the production of high levels of NO in a wide variety of cells, including macrophages, and is regulated primarily at the transcriptional level (20, 21). Many signaling pathways and inducible transcription factors, including Akt, NF-κB, JNK and p38 mitogen-activated protein kinase (p38), cAMP response element-binding protein (CREB), and CCAAT/enhancer-binding protein-β, have been implicated in iNOS activation (22–26). iNOS is important for host defense against *P. gingivalis* infection. When orally infected with *P. gingivalis*, iNOS-deficient mice exhibit more extensive soft tissue damage and alveolar bone loss (17, 18) and display an impaired ability to kill *P. gingivalis* (3, 16). As this phenotype of iNOS-deficient mice after *P. gingivalis* infection is strikingly similar to the one we previously observed in DIO mice after *P. gingivalis* infection (3), we hypothesized that DIO impairs the innate immune response to bacterial infection via a mechanism that includes disrupting iNOS. In the present study we tested this hypothesis, and show that the changes observed in bone marrow macrophages (BMMΦ) from DIO mice can be reproduced in vitro after exposing FFAs to BMMΦ from lean mice.

Results

DIO Blunts *P. gingivalis*-Induced iNOS Expression. To determine whether impaired bacterial clearance in DIO mice (3) is associated with dysregulated NO production upon infection with *P. gingivalis*, we analyzed the expression of iNOS-in infected tissue from lean mice and from mice with DIO, using an in vivo murine calvarial model (27). iNOS expression was dramatically attenuated in DIO mice at day 3 after infection in comparison with lean mice (Fig. 1*A*). BMMΦ from DIO mice exhibited severe impairment of iNOS induction at the protein level (Fig. 1*B*, *i*) and at the mRNA level (Fig. 1*B*, *ii*) after *P. gingivalis* infection compared with BMMΦ from lean mice.

TLR2 Is Disrupted in Mice with DIO. As *P. gingivalis* is a major TLR2 ligand by which macrophages sense infection, we asked whether

Author contributions: S.A. designed research; Q.Z. and S.A. performed research; Q.Z. and S.A. contributed new reagents/analytic tools; Q.Z., S.E.L., and S.A. analyzed data; and Q.Z., S.E.L., and S.A. wrote the paper.

The authors declare no conflict of interest.

Freely available online through the PNAS open access option.

[1]To whom correspondence may be addressed. E-mail: samar@bu.edu or sleeman@bu.edu.

This article contains supporting information online at www.pnas.org/cgi/content/full/0904412106/DCSupplemental.

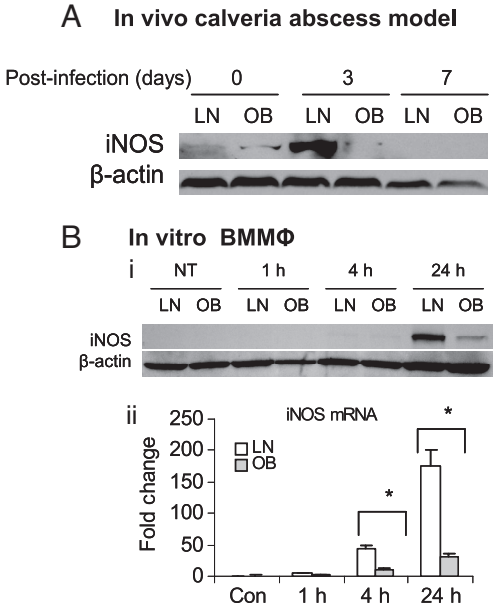

Fig. 1. DIO inhibits the induction of iNOS and cytokines after *P. gingivalis* infection. (*A*) In vivo studies: lean (*LN*) and obese (*OB*) mice were infected with *P. gingivalis* using a murine calvarial model for 24 h, 3 d, or 7 d; the induction of iNOS in infected tissues was determined by Western blot. (*B*) In vitro studies: BMMΦ from lean mice and mice with DIO were stimulated with *P. gingivalis* for 1, 4, and 24 h or left untreated (*NT*); the induction of iNOS was measured by Western blot (*i*) and real-time PCR (*ii*). Each result is representative of 3 independent experiments. Data are expressed as mean ± SEM ($n = 3$; $^*P < 0.05$).

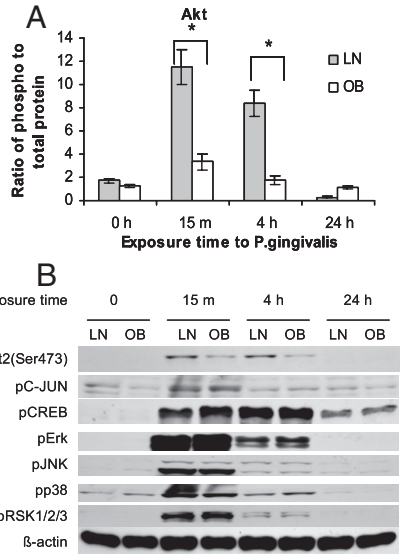

Fig. 3. DIO inhibits Akt phosphorylation after *P. gingivalis* infection. (*A*) Ratio of pAkt to total Akt was measured by Bio-Plex phosphoprotein array. BMMΦ from LN and OB mice were stimulated with *P. gingivalis* for 0, 15 min, 4 h, and 24 h; both pAkt and total Akt were quantitated in the cell lysates. Data are expressed as mean ± SEM ($n = 3$; $^*P < 0.05$). The data of the other 20 kinases that showed little changes or changes that were unconfirmed by Western blot are shown in Fig. S2. (*B*) Phosphor-protein of kinases detected by Western blot using the same cell lysates prepared for Bio-Plex phosphoprotein array. Each result represents one of 3 independent experiments.

the reduced iNOS and cytokine induction observed in DIO mice after *P. gingivalis* infection was caused by the disruption of the TLR2 signaling pathway. We first investigated *TLR2* expression in BMMΦ from lean mice and from mice with DIO. As expected, *TLR2* mRNA expression in BMMΦ from lean mice was approximately threefold higher than that in BMMΦ from mice with DIO (Fig. 2*A*); *TLR4* showed a slight significance between these 2 types of cells whereas *TLR6* and *TLR7* did not exhibit any significant difference [supporting information (SI) Fig. S1].

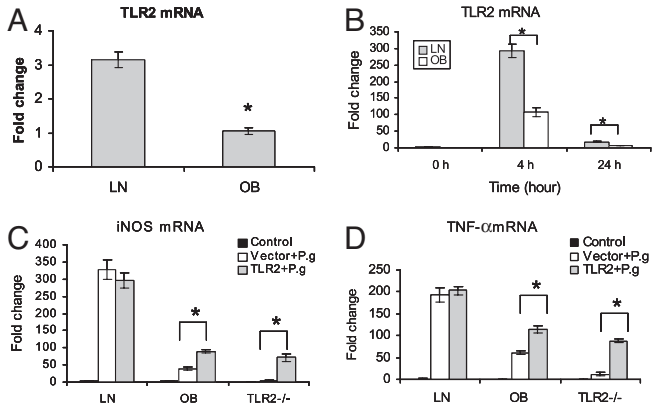

Fig. 2. DIO disrupts TLR2 signaling. (*A*) Total RNA was purified from untreated BMMΦ either from lean (*LN*) or obese (*OB*) mice; *TLR2* mRNA was measured by real-time RT-PCR. (*B*) BMMΦ from lean and obese mice were infected with *P. gingivalis* for 0, 4, and 24 h, and the *TLR2* mRNA was detected by real-time RT-PCR. (*C* and *D*) BMMΦ from lean, obese, and *TLR2-/-* mice were first transfected with murine full-length cDNA or empty vector for 4 h, then stimulated with PBS solution (control) or *P. gingivalis* overnight; total RNA was purified from the cells and the mRNA of *iNOS* (*C*), and *TNF-α* (*D*) was measured using real-time RT-PCR. Data are expressed as mean ± SEM ($n = 3$; $^*P < 0.05$).

After *P. gingivalis* induction, *TLR2* was fourfold greater in lean BMMΦ than in BMMΦ with DIO (Fig. 2*B*), whereas only a moderate significance was observed for *TLR4* and *TLR7*. *TLR6* did not show any significant difference. Next we tested whether transfection with exogenous *TLR2* could restore in DIO mouse BMMΦ the induction of *iNOS* and *TNF-α*. BMMΦ from lean mice, mice with DIO, and *TLR2-/-* mice were transfected with full-length mouse *TLR2* cDNA or empty vector, then infected with *P. gingivalis* for 4 h. The mRNA levels of *iNOS* (Fig. 2*C*) and *TNF-α* (Fig. 2*D*) measured by real-time PCR were increased significantly in *TLR2*-transfected BMMΦ from mice with DIO and from *TLR2-/-* mice, but the mRNA levels were unable to be restored as high as those seen in BMMΦ from normal WT mice.

DIO Disrupts Akt Phosphorylation in BMMΦ After *P. gingivalis* Infection. To determine the signaling pathway downstream of TLR2, we tested the effect of DIO on protein phosphorylation. BMMΦ from mice with DIO and lean mice were challenged with *P. gingivalis* for 15 min, 4 h, or 24 h. A set of 21 phosphorylated proteins (*p*-Akt, *p*-ERK1/2, *p*-GSK3α/β, *p*-JNK, *p*-p38MAPK, *p*-p70S6 kinase, *p*-p90RSK, *p*-TrkA, *p*-NF-κB p65, *p*-PDGFR, *p*-p53, *p*-STAT6, *p*-cJUN, *p*-CREB, *p*-HSP27, *p*-IRS1, *p*-MEK1, *p*-ATF2, *p*-Histone H3, *p*-STAT2, and *p*-STAT3) and their corresponding total proteins were analyzed using Bio-Plex phosphorylation protein array. The phosphorylation of Akt at Ser-473 was found strongly reduced in BMMΦ with DIO compared with their lean counterparts at 15 min and 4 h after infection with *P. gingivalis* (Fig. 3*A*). The difference of Akt phosphorylation was further confirmed by Western blot using the same protein samples as for Bio-Plex phosphorylation protein array (Fig. 3*B*). The phospho-proteins of *p*-JNK, *p*-p38MAPK, *p*-cJUN, *p*-CREB, *p*-p90RSK, and *p*-Erk were also diminished to a certain extent in BMMΦ from obese mice upon *P. gingivalis* infection (Fig. S2), but showed no difference when they were detected by Western blot (Fig. 3*B*).

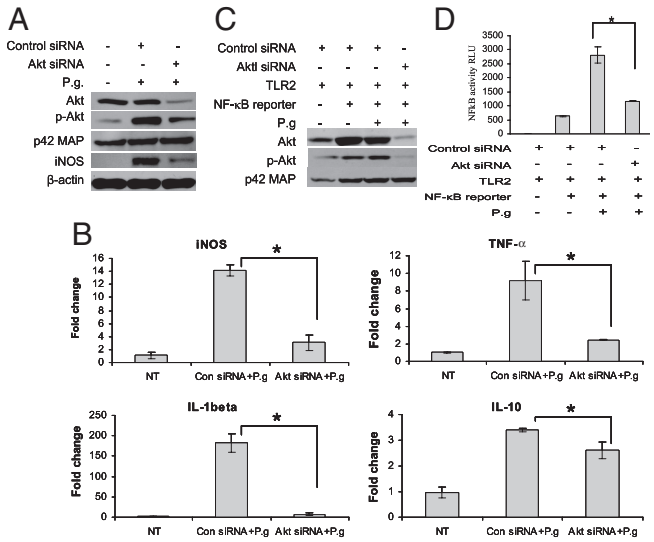

Fig. 4. *Akt* silencing with siRNA diminishes the induction of iNOS and cytokines, and inhibits NF-κB activity. (*A* and *B*) BMMΦ from 4-week-old C57BL/6J mice were transfected with siRNA for *Akt* or control siRNA and subsequently stimulated with *P. gingivalis* for 4 h; Total protein and RNA were extracted from cells and subjected to Western blot (*A*) and real time RT-PCR (*B*). (*C* and *D*) HEK293 cells were first transfected with siRNA for *Akt* or control siRNA, then transfected with NF-κB luciferase reporter along with a human TLR2 expression vector; After 4 h, cells were infected with *P. gingivalis* and incubated overnight. Cell lysates were harvested and subjected to Western blot (*C*) and luciferase assay (*D*). Each result represents 3 independent experiments. Data are expressed as mean ± SEM ($n = 3$; $*P < 0.05$).

Disruption of Akt Phosphorylation Is Responsible for Attenuated iNOS Induction and NF-κB Activation After *P. gingivalis* Infection. To test the influence of the Akt on iNOS and cytokine induction by *P. gingivalis*, we investigated the iNOS and cytokine expression in BMMΦ rendered *Akt*-deficient by siRNA approach. *Akt* silencing specifically inhibited Akt, whereas the non-target p42 MAPK remained unchanged (Fig. 4*A*). As the result of a dramatic reduction of total Akt, much less phosphorylated Akt (Ser-473) was induced in *Akt* silenced cells after *P. gingivalis* infection compared with cells transfected with control siRNA (Fig. 4*A*). After *Akt* silencing, the induction of iNOS by *P. gingivalis* was greatly reduced at both the protein level (Fig. 4*A*) and the mRNA level (Fig. 4*B*) in mouse BMMΦ. The expression of both proinflammatory cytokines (*TNF-α* and *IL-1*) and anti-inflammatory cytokine (*IL-10*) after infection with *P. gingivalis* was also inhibited in BMMΦ transfected with siRNA for *Akt* (Fig. 4*B*). Because NF-κB is critical for iNOS and cytokine expression, we tested the effect of *Akt* silencing on NF-κB activation in HEK 293 cells, which do not produce mediators such as TNF-α and IL-10 capable of inducing a secondary NF-κB response. The HEK293 cells were first transfected with Akt siRNA to silence *Akt*, then transiently transfected with *NF-κB* luciferase reporter along with a human *TLR2* expression vector (ligand for *P. gingivalis*) and followed by *P. gingivalis* infection. Transfection with siRNA significantly suppressed Akt expression in HEK293 cells and subsequently reduced the phospho-Akt level after *P. gingivalis* infection (Fig. 4*C*). The gene silencing of *Akt* resulted in a dramatic reduction of NF-κB activation after *P. gingivalis* infection (Fig. 4*D*).

CTMP Inhibits Akt Phosphorylation After *P. gingivalis* Infection. Knowing that Akt phosphorylation is negatively regulated by phosphatase and tensin homologue (PTEN) (28), protein phosphatase 2A (PP2A) (29), and CTMP (30, 31), we investigated whether DIO-associated inhibition of Akt phosphorylation is caused by abnormal expression of any of these proteins. Only CTMP was found to be significantly higher in BMMΦ from DIO mice than in BMMΦ from their lean counterparts (Fig. 5*A*), whereas PTEN and PP2A levels did not differ between BMMΦ from lean and DIO mice.

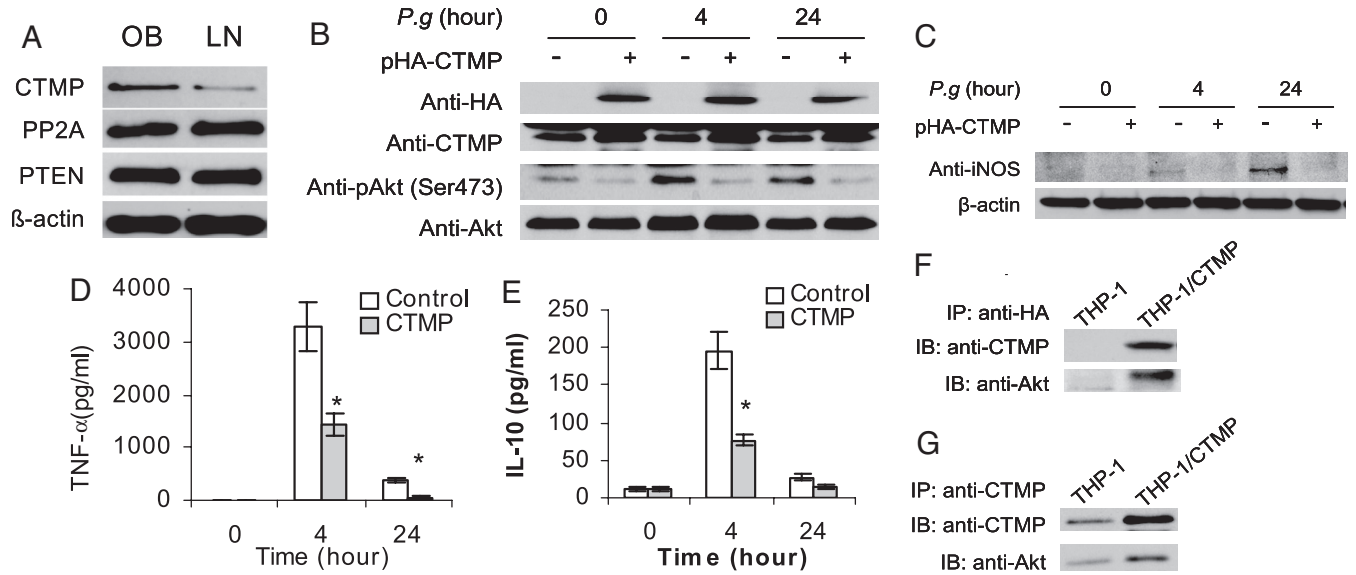

Fig. 5. CTMP induced by DIO inhibits Akt phosphorylation and attenuates innate immune responses. (*A*) Total protein was extracted from un-stimulated BMMΦ isolated from obese (*OB*) and lean (*LN*) mice. CTMP, PP2A, and PTEN were detected by using Western blot. (*B*) CTMP suppresses Akt phosphorylation. THP-1 cells were stably transfected with HA-tagged *CTMP* or empty vector and then infected with *P. gingivalis* for 0, 4, and 24 h, and Western blots were performed using total cell lysates. (*C–E*) CTMP inhibits innate immune responses. THP-1 cells stably transfected with *CTMP* or empty vector were infected with *P. gingivalis* for 0, 4, and 24 h; the induction of iNOS was detected in cell lysates by Western blot (*C*), and the release of TNF-α (*D*) or IL-10 (*E*) was measured by ELISA using cell culture supernatants. (*F* and *G*) CTMP physically interacts with Akt. THP-1 cells were stably transfected with *CTMP* or empty vector. After serum starvation (24 h), total proteins were extracted and immunoprecipitated using either anti-HA (*F*) or anti-CTMP (*G*) antibodies; Akt was analyzed by using an antibody against total Akt by Western blot. Each image represents one of the triplicate results. Data are expressed as mean ± SEM ($n = 3$; $*P < 0.05$).

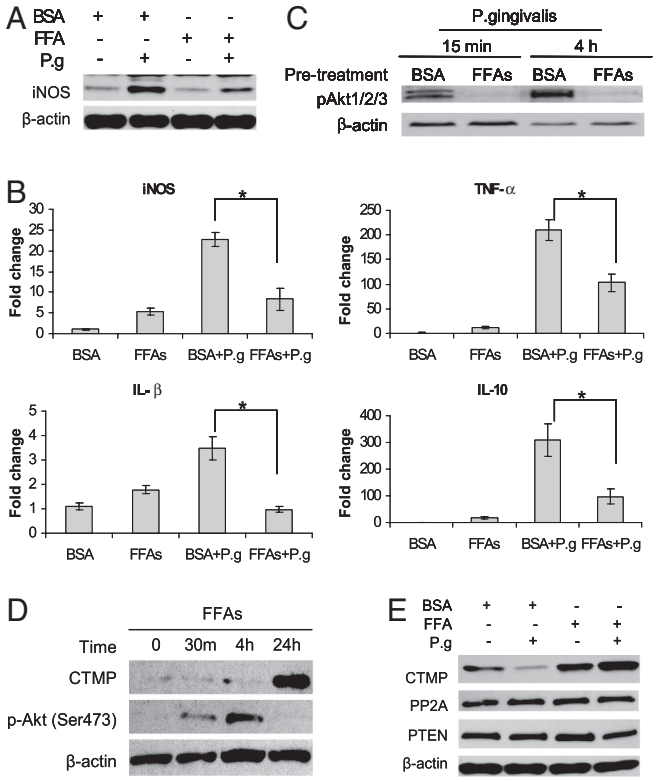

Fig. 6. FFAs inhibit the innate immune response to *P. gingivalis*. BMMΦ from 4-week-old C57BL/6J mice were pretreated with BSA or FFAs for 24 h, followed by stimulation with FFAs or *P. gingivalis* for 4 h; the induction of iNOS and cytokines was detected by Western blot (*A*) and/or real-time PCR (*B*). (*C*) BMMΦ were pretreated with FFAs for 24 h, followed by infection with *P. gingivalis* for 15 min or 4 h; phosphor-Akt was detected by Western blot. (*D*) BMMΦ from 4-week-old C57BL/6J mice were treated with FFAs for 0, 30 min, 4 h, and 24 h, and the induction of CTMP or pAkt was detected by Western blot. (*E*) BMMΦ from 4-week-old C57BL/6J mice were pretreated with BSA or FFAs for 24 h and stimulated with FFAs or *P. gingivalis* overnight; CTMP, PP2A, and PTEN were detected by Western blot. Each image represents one of the triplicate results. Data are expressed as mean ± SEM ($n = 3$; $^*P < 0.05$).

To determine whether the increased CTMP directly causes the inhibition of Akt phosphorylation, we established a CTMP-overexpressing THP-1 stable cell line. The exogenous HA-tagged CTMP was successfully expressed in stably transfected THP-1 cells (Fig. 5*B*). The overexpression of CTMP significantly suppressed Akt phosphorylation in THP-1 cells, both at baseline level and 4 h or 24 h after infection with *P. gingivalis* (Fig. 5*B*). In addition, after *P. gingivalis* infection, the induction of iNOS (Fig. 5*C*), TNF-α (Fig. 5*D*), and IL-10 (Fig. 5*E*) was significantly reduced in THP-1 cells stably transfected with *CTMP* compared with cells transfected with empty vector. An immunoprecipitation further demonstrated that Akt co-precipitated with CTMP (Fig. 5 *F* and *G*).

FFAs Inhibit the Induction of iNOS, Suppress Akt Phosphorylation, and Induce CTMP Expression. Given that FFAs are elevated in serum of obese individuals and play an important role in the pathogenesis of metabolic syndrome (32–34), we tested whether palmitate and oleate, 2 of the most abundant nutritional FFAs, were responsible for the attenuated *P. gingivalis*-induced iNOS or cytokine in mice with DIO. The induction of iNOS by *P. gingivalis* was much higher than that by FFAs (Fig. 6*A*). However, when BMMΦ were pretreated with FFAs for 24 h, the induction of iNOS after *P. gingivalis* infection was significantly attenuated at both the protein level (Fig. 6*A*) and the mRNA level (Fig. 6*B*). This

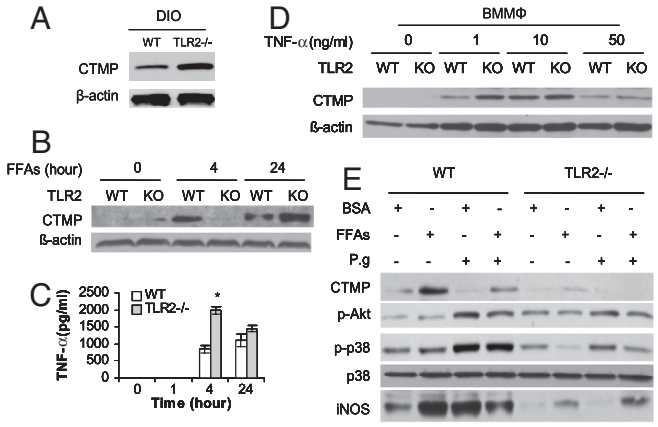

Fig. 7. TLR2 modulates CTMP expression. (*A*) Total proteins of BMMΦ from WT and *TLR2-/-* obese mice were extracted and the CTMP levels in BMMΦ were detected by Western blot. (*B* and *C*) BMMΦ from 4-week-old WT or *TLR2-/-* mice were stimulated with FFAs for 0, 4, and 24 h; the induction of CTMP was analyzed using Western blot (*B*) and the TNF-α in cell culture supernatants were measured by ELISA (*C*). (*D*) BMMΦ from 4-week-old WT or *TLR2-/-* mice were stimulated with TNF-α at indicated concentrations for 4 h; CTMP in whole-cell lysate was analyzed using Western blot. (*E*) BMMΦ from 4-week-old WT or *TLR2-/-* mice were pretreated with BSA or FFAs for 4 h, then washed and infected with *P. gingivalis* or stimulated with FFAs overnight; cell lysates were analyzed by Western blot. Each result represents 3 independent experiments. Data are expressed as mean ± SEM ($n = 3$; $^*P < 0.05$).

inhibition was also observed for both proinflammatory (*TNF-α*, *IL-1β*) and anti-inflammatory cytokines (*IL-10*; Fig. 6*B*).

Furthermore, pretreatment of BMMΦ from lean mice with a mixture of oleate and palmitate led to significant suppression of Akt phosphorylation 15 min and 4 h after infection with *P. gingivalis* (Fig. 6*C*).

To determine whether FFAs induces CTMP, we demonstrated that stimulation with FFAs dramatically elevated CTMP in BMMΦ after 4 h and 24 h, and this increase in CTMP was associated with complete inhibition of Akt phosphorylation at 24 h (Fig. 6*D*). In addition, stimulation with *P. gingivalis* alone decreased CTMP in BMMΦ, but the CTMP level was dramatically elevated in BMMΦ pretreated with FFAs and infected with *P. gingivalis* compared with BMMΦ pretreated with BSA (Fig. 6*E*). Stimulation with either *P. gingivalis* or FFAs alone or in combination had little effect on PTEN and PP2A expression (Fig. 6*E*).

TLR2 Regulates CTMP Expression. Because TLR2 is suppressed in mice with DIO, we tested whether the elevated CTMP in mice with DIO is related to the disruption of TLR2. In fact, CTMP levels in BMMΦ from *TLR2-/-* mice with DIO were significantly higher than in BMMΦ from WT mice with DIO (Fig. 7*A*), suggesting that TLR2 negatively regulates CTMP expression in mice with DIO.

To further test whether TLR2 negatively regulates CTMP induction by FFAs, BMMΦ from WT and *TLR2-/-* mice were treated with FFAs for 0, 4, and 24 h and CTMP in cell lysates were measured. To our surprise, CTMP induction by FFAs was significantly reduced at 4 h, but increased at 24 h in *TLR2-/-* BMMΦ relative to WT BMMΦ (Fig. 7*B*), suggesting that TLR2 is critical for the induction of CTMP by FFAs and plays an important role in regulating the increased expression of CTMP in a secondary response.

As FFAs are able to induce more TNF-α in *TLR2-/-* BMMΦ than in WT BMMΦ (Fig. 7*C*), we investigated whether the stronger secondary response of CTMP in *TLR2-/-* BMMΦ is caused by TNF-α signaling. BMMΦ were treated with TNF-α for 4 h to detect the early CTMP response. At the concentration of

1 ng/mL, TNF-α induced more CTMP in *TLR2*-/- BMMΦ compared with WT BMMΦ; however, there was no significant difference of CTMP expression between these 2 types of cells when the concentration of TNF-α was increased to 10 or 50 ng/mL (Fig. 7*D*). The induction of CTMP was much weaker in response to 50 ng/mL in both *TLR2*-/- and WT BMMΦ because this high concentration of TNF-α induced cell apoptosis (Fig. S3). These data indicate that TLR2 negatively regulates CTMP induction by the low concentration of TNF-α.

To further investigate the combined role of TLR2 and FFAs in the regulation of Akt, CTMP, and iNOS in response to *P. gingivalis* infection, BMMΦ from WT and *TLR2*-/- mice were pretreated with FFAs or BSA for 4 h and then infected with *P. gingivalis* or treated with FFAs overnight. When compared with BSA-pretreated cells, the pretreatment of WT BMMΦ with FFAs was associated with significantly elevated CTMP, reduced Akt phosphorylation, and attenuated iNOS induction after *P. gingivalis* infection (Fig. 7*E*). However, in *TLR2*-/- BMMΦ, the pretreatment with FFAs led to a significantly diminished p38 phosphorylation and elevated iNOS induction, yet had little effect on CTMP expression or Akt phosphorylation (Fig. 7*E*).

Discussion

The present study extends our knowledge of the changes in signaling mechanisms that occur after feeding animals a high-fat diet that led to an impaired ability of their macrophages to respond effectively to bacteria and mount an adequate inflammatory response (3). Both DIO and FFAs attenuate iNOS and cytokine induction when mice or BMMΦ are challenged with *P. gingivalis*. The impaired induction of iNOS and cytokines in mice with DIO may explain the compromised immunity observed in obese individuals (3, 4, 17). In addition, both DIO and FFAs suppress proinflammatory cytokines TNF-α and IL-1β and the anti-inflammatory cytokine IL-10, indicating that DIO may directly reduce TNF-α and IL-1β expression, whereas the reduction of IL-10 may be only a reaction to the reduced proinflammatory process.

To investigate the mechanisms whereby DIO attenuates iNOS and cytokine induction, we demonstrated that the disruption of Akt phosphorylation by DIO or FFAs occurs and is responsible for the inhibition of iNOS and cytokine induction after *P. gingivalis* infection. The serine/threonine kinase Akt is a central node in cell signaling downstream of growth factors, cytokines, and other cellular stimuli. Akt activation is regulated by PI3K-dependent second messenger molecules (35). In the obesity-induced insulin resistant condition, JNK and p70S6K are activated and phosphorylate insulin receptor substrate (IRS) proteins, which diminish the insulin-induced tyrosine phosphorylation of IRS proteins and thereby impair PI3-kinase/Akt activation (36). However, the disruption of *P. gingivalis*-induced Akt phosphorylation is not caused by the diminished phosphorylation of the global network of IRS proteins, because activation of JNK and p70S6K are not affected in DIO BMMΦ after *P. gingivalis* infection. Therefore, we explored the ability of DIO and FFAs to induce molecules such as CTMP, PP2A, and PTEN (28–31). We found that CTMP is elevated in BMMΦ from mice with DIO, and directly inhibits Akt phosphorylation. In addition, FFAs, whose levels are elevated in serum from obese individuals (32, 34), also induce CTMP in BMMΦ, leading to the suppression of *P. gingivalis*-induced Akt phosphorylation, and inhibit iNOS and cytokine induction. CTMP can bind specifically to the carboxyl-terminal regulatory domain of Akt at the plasma membrane, resulting in the inhibition of phosphorylation on serine 473 and threonine 308 (30). It is possible that the elevated cellular pool of CTMP in BMMΦ from obese mice and in FFA-treated cells physically interacts with Akt, thereby leading to the suppression of Akt phosphorylation after *P. gingivalis* infections.

After demonstrating that DIO and FFAs disrupt Akt phosphorylation and diminish host innate immune responses via inducing CTMP, we next sought to determine the signaling pathways by which DIO or FFAs induce CTMP in BMMΦ. TLRs have been reported to play important roles in both innate immunity and lipid-induced metabolic syndromes (15, 37, 38). As an immune sensor for *P. gingivalis* (11–14, 39), TLR2 also recognizes lipids, and mediates the initial events of FFA-induced insulin resistance (15). The fatty acid residue at the glycerol position in the triacylated lipoprotein from *P. gingivalis* has been identified as a determinant element that can be recognized by TLR2 (40). In this regard, we tested whether TLR2 plays a role in the induction of CTMP in mice with DIO or in FFA-exposed BMMΦ. Whereas in lean mice TLR2 functions as a negative regulator of CTMP, to our surprise, in mice with DIO, TLR2 functioning is significantly impaired. Our evidence supports that the high level of CTMP in mice with DIO results from the TLR2 inability to respond to its ligands, as in lean BMMΦ FFAs, induction of CTMP is dependent on TLR2, and in DIO BMMΦ, the transfection on WT TLR2 partially restores the malfunction. However, *TLR2*-/- BMMΦ can express CTMP only after longer (24 h) exposure of FFAs. As FFAs can activate TLR4 to induce cytokines (38), and as the induction of TNF-α by FFAs is stronger in *TLR2*-/- BMMΦ than that in WT BMMΦ (Fig. 6C), we hypothesize that, with a dysfunctional TLR2 in DIO mice, FFAs activate TLR4 to induce TNF-α, which in turn increases the expression of CTMP. To test this hypothesis, we investigated if TNF-α can induce CTMP. As expected, TNF-α has the ability to induce CTMP in BMMΦ, but importantly TLR2 limits the induction of CTMP by low concentration of TNF-α (1 ng/mL). These results can explain why DIO induces more CTMP in *TLR2*-/- BMMΦ than in WT controls, although FFAs induction of CTMP is dependent on TLR2. We therefore conclude that FFAs induces CTMP via TLR2 during the early stage of DIO, but at a later stage, TLR2 is disrupted by chronic FFA stimulation, permitting CTMP to be significantly increased by TNF-α in DIO mice. The increase CTMP in DIO mice further leads to the inhibition of Akt activation and finally results in immune suppression.

In summary (Fig. S4), DIO is able to elevate TNF-α induced CTMP by disrupting TLR2, whereas FFAs use TLR2 directly to induce CTMP in BMMΦ. The elevated pool of CTMP in BMMΦ plays an important role in the suppression of Akt phosphorylation, which in turn leads to the inhibition of host innate immune responses, such as reduced induction of iNOS and cytokines. These data unveil a link between obesity and innate immune response with profound implications for the design of therapies aimed at reducing clinical sequelae of obesity.

Materials and Methods

Bacteria and Cell Lines. All bacterial cloning constructs used *Escherichia coli* strain DH5α (Invitrogen). *P. gingivalis* A7436 (American Type Culture Collection) was cultured anaerobically in Schaedler broth (Becton Dickinson) as described previously (14, 41). THP-1 cells (American Type Culture Collection) were grown in RPMI 1640 supplemented with 10% FBS (Invitrogen). HEK 293 cells (Invivogen) and the RetroPack PT67 cells (Clontech) were cultured in DMEM supplemented with 10% FBS. All cell cultures were maintained in a 37 °C humidified atmosphere containing 5% CO_2.

Animal Experiment. C57BL/6J and TLR2 knockout (*TLR2-/-*) mice were obtained from Jackson Laboratories and fed a high-fat diet for 16 weeks as described previously (3). Mice infection with *P. gingivalis* was conducted by using mouse calvaria model (27).

Macrophage Isolation and Treatment. BMMΦ isolated from hind legs of mice were cultured according to a previous study (42). FFAs (oleate and palmitate mixture; Sigma-Aldrich) were dissolved in 95% ethanol at 60 °C and then mixed with pre-warmed BSA (10%) to yield a stock concentration of 8 mM. The endotoxin content of BSA-fatty acid conjugates was ≤0.04 ng/mL, measured with a chromogenic *Limulus* amebocyte lysate assay (Cambrex). Cells were treated with FFAs at a final concentration of 400 μM. To infect the cells, *P. gingivalis* was added with multiplicities of infection of 10:1 as previously described (14).

Plasmid Construction, DNA Transfection, and Luciferase Reporter Assay. Mouse *TLR2* cDNA was generated by RT-PCR from mouse cDNA library and sub-cloned into plasmid pcDNA3.1 (Invitrogen). A human *TLR2* cDNA construct was provided by X. Tang (Boston, MA). NF-κB luciferase vectors (pNF-κB-Luc) were purchased from Panomics. DNA transfection was conducted using Lipofectamine 2000 reagent (Invitrogen). Luciferase activity was measured using a dual-luciferase reporter assay kit (Promega).

Construction of Retroviral Vectors and Transduction of THP-1 Cells. The human full-length cDNA of *CTMP* was obtained by RT-PCR using HA-tagged primers and inserted into the retroviral vector pMSCVneo (Clontech). The recombinant retroviral vector was transfected into the packaging cell line PT67 by Clonfectin transfection reagent (Clontech). After 48 h, stable PT67 cells were selected with 1 mg/mL neomycin. The supernatants of stable PT67 cells producing retroviruses were used to transduce THP-1 cells and the stably expressing HA-tagged CTMP THP-1 cells were selected with 1 mg/mL neomycin.

RNA Preparation and Quantitative Real-Time PCR. Total RNA extraction, reverse transcription, and real-time PCR were conducted as described in our previous study (13).

RNA Interference. Transfection of SignalSilence *Akt* siRNA (Cell Signaling) was performed using GeneSilencer siRNA transfection reagent (Gene Therapy Systems). siGuard RNase inhibitor (Gene Therapy Systems) was added to the culture just before transfection. siRNA transfection was repeated 24 h after the first transfection. The subsequent experiments were performed 48 h after the second transfection.

Bio-Plex Phosphoprotein Array. Cell lysates from BMMΦ treated with or without *P. gingivalis* were analyzed using a Bio-Plex phosphoprotein reagent kit with coupled beads in the Bio-Plex 200 system (Bio-Rad) as described in the manufacturer's instruction manual.

ELISA. Concentrations of cytokines were determined by BD Biosciences-PharMingen ELISA kits for assay of human TNF-α, human IL-10, mouse TNF-α, and mouse IL-10.

Immunoprecipitation and Western Blot. CTMP was immunoprecipitated from THP-1 cell by using anti-HA or anti-CTMP antibodies. Western blot were performed using Abs against Akt, *p*-Akt (Ser-473), CTMP, PTEN, PP2A, pC-JUN, pCREB, pERK, pJNK, *p*-p38, pRSK1/2/3, p42 MAPK (all from Cell Signaling), iNOS, *p*-Akt1/2/3, β-actin, and HRP-conjugated IgG (all from Santa Cruz Biotechnology).

Statistical Analysis. Statistical analysis was performed with JMP statistical software (SAS Institute). Two-tailed Student *t* test was used to evaluate the significance of differences. $P \leq 0.05$ was regarded as statistically significant.

ACKNOWLEDGMENTS. This work was supported by Grant DE15989 from the National Institute of Dental and Craniofacial Research (to S.A.).

1. Espejo B, et al. (2003) Obesity favors surgical and infectious complications after renal transplantation. *Transplant Proc* 35:1762–1763.
2. Canturk Z, Canturk NZ, Cetinarslan B, Utkan NZ, Tarkun I (2003) Nosocomial infections and obesity in surgical patients. *Obes Res* 11:769–775.
3. Amar S, Zhou Q, Shaik-Dasthagirisaheb Y, Leeman S (2007) Diet-induced obesity in mice causes changes in immune responses and bone loss manifested by bacterial challenge. *Proc Natl Acad Sci USA* 104:20466–20471.
4. Smith AG, Sheridan PA, Harp JB, Beck MA (2007) Diet-induced obese mice have increased mortality and altered immune responses when infected with influenza virus. *J Nutr* 137:1236–1243.
5. Perez-Echarri N, et al. (2008) Differential inflammatory status in rats susceptible or resistant to diet-induced obesity: effects of EPA ethyl ester treatment. *Eur J Nutr* 47:380–386.
6. Kanbay A, Kokturk O, Ciftci TU, Tavil Y, Bukan N (2008) Comparison of serum adiponectin and tumor necrosis factor-alpha levels between patients with and without obstructive sleep apnea syndrome. *Respiration* 76:324–330.
7. Lee FY, et al. (1999) Phenotypic abnormalities in macrophages from leptin-deficient, obese mice. *Am J Physiol* 276:C386–C394.
8. Mancuso P, et al. Leptin-deficient mice exhibit impaired host defense in Gram-negative pneumonia. *J Immunol* 168:4018–4024.
9. Mito N, Hosoda T, Kato C, Sato K (2000) Change of cytokine balance in diet-induced obese mice. *Metabolism* 49:1295–1300.
10. Cousin B, Andre M, Casteilla L, Penicaud L (2001) Altered macrophage-like functions of preadipocytes in inflammation and genetic obesity. *J Cell Physiol* 186:380–386.
11. Burns E, Bachrach G, Shapira L, Nussbaum G (2006) Cutting edge: TLR2 is required for the innate response to Porphyromonas gingivalis: activation leads to bacterial persistence and TLR2 deficiency attenuates induced alveolar bone resorption. *J Immunol* 177:8296–8300.
12. Hajishengallis G, Wang M, Bagby GJ, Nelson S (2008) Importance of TLR2 in early innate immune response to acute pulmonary infection with Porphyromonas gingivalis in mice. *J Immunol* 181:4141–4149.
13. Zhou Q, Amar S (2007) Identification of signaling pathways in macrophage exposed to Porphyromonas gingivalis or to its purified cell wall components. *J Immunol* 179:7777–7790.
14. Zhou Q, Desta T, Fenton M, Graves DT, Amar S (2005) Cytokine profiling of macrophages exposed to Porphyromonas gingivalis, its lipopolysaccharide, or its FimA protein. *Infect Immun* 73:935–943.
15. Senn JJ (2006) Toll-like receptor-2 is essential for the development of palmitate-induced insulin resistance in myotubes. *J Biol Chem* 281:26865–26875.
16. Gyurko R, et al. (2003) Mice lacking inducible nitric oxide synthase demonstrate impaired killing of Porphyromonas gingivalis. *Infect Immun* 71:4917–4924.
17. Alayan J, et al. (2006) Deficiency of iNOS contributes to Porphyromonas gingivalis-induced tissue damage. *Oral Microbiol Immunol* 21:360–365.
18. Fukada SY, et al. (2008) iNOS-derived nitric oxide modulates infection-stimulated bone loss. *J Dent Res* 87:1155–1159.
19. Nathan C (1992) Nitric oxide as a secretory product of mammalian cells. *FASEB J* 6:3051–3064.
20. Lowenstein CJ, et al. (1993) Macrophage nitric oxide synthase gene: two upstream regions mediate induction by interferon gamma and lipopolysaccharide. *Proc Natl Acad Sci USA* 90:9730–9734.
21. Xie QW, Whisnant R, Nathan C (1993) Promoter of the mouse gene encoding calcium-independent nitric oxide synthase confers inducibility by interferon gamma and bacterial lipopolysaccharide. *J Exp Med* 177:1779–1784.
22. Oh JH, Lee TJ, Park JW, Kwon TK (2008) Withaferin A inhibits iNOS expression and nitric oxide production by Akt inactivation and down-regulating LPS-induced activity of NF-kappaB in RAW 264.7 cells. *Eur J Pharmacol* 599:11–17.
23. Lee SA, Park SH, Kim BC (2008) Raloxifene, a selective estrogen receptor modulator, inhibits lipopolysaccharide-induced nitric oxide production by inhibiting the phosphatidylinositol 3-kinase/Akt/nuclear factor-kappa B pathway in RAW264.7 macrophage cells. *Mol Cells* 26:48–52.
24. Kang JS, et al. (2007) Equol inhibits nitric oxide production and inducible nitric oxide synthase gene expression through down-regulating the activation of Akt. *Int Immunopharmacol* 7:491–499.
25. Guan Z, Baier LD, Morrison AR (1997) p38 mitogen-activated protein kinase down-regulates nitric oxide and up-regulates prostaglandin E2 biosynthesis stimulated by interleukin-1beta. *J Biol Chem* 272:8083–8089.
26. Eberhardt W, Pluss C, Hummel R, Pfeilschifter J (1998) Molecular mechanisms of inducible nitric oxide synthase gene expression by IL-1beta and cAMP in rat mesangial cells. *J Immunol* 160:4961–4969.
27. Graves DT, et al. (2005) Inflammation is more persistent in type 1 diabetic mice. *J Dent Res* 84:324–328.
28. Wan X, Helman LJ (2003) Levels of PTEN protein modulate Akt phosphorylation on serine 473, but not on threonine 308, in IGF-II-overexpressing rhabdomyosarcomas cells. *Oncogene* 22:8205–8211.
29. Sato S, Fujita N, Tsuruo T (2000) Modulation of Akt kinase activity by binding to Hsp90. *Proc Natl Acad Sci USA* 97:10832–10837.
30. Maira SM, et al. (2001) Carboxyl-terminal modulator protein (CTMP), a negative regulator of PKB/Akt and v-Akt at the plasma membrane. *Science* 294:374–380.
31. Hwang SK, et al. (2007) Lentivirus-mediated carboxyl-terminal modulator protein gene transfection via aerosol in lungs of K-ras null mice. *Gene Ther* 14:1721–1730.
32. Pankow JS, et al. (2004) Fasting plasma free fatty acids and risk of type 2 diabetes: the atherosclerosis risk in communities study. *Diabetes Care* 27:77–82.
33. Mook S, Halkes CC, Bilecen S, Cabezas MC (2004) In vivo regulation of plasma free fatty acids in insulin resistance. *Metabolism* 53:1197–1201.
34. Shankar SS, Steinberg HO (2005) FFAs: do they play a role in vascular disease in the insulin resistance syndrome? *Curr Diab Rep* 5:30–35.
35. Franke TF, Cantley LC (1997) Apoptosis: a Bad kinase makes good. *Nature* 390:116–117.
36. Asano T, et al. (2007) Role of phosphatidylinositol 3-kinase activation on insulin action and its alteration in diabetic conditions. *Biol Pharm Bull* 30:1610–1616.
37. Kim F, et al. (2007) Toll-like receptor-4 mediates vascular inflammation and insulin resistance in diet-induced obesity. *Circ Res* 100:1589–1596.
38. Shi H, et al. (2006) TLR4 links innate immunity and fatty acid-induced insulin resistance. *J Clin Invest* 116:3015–3025.
39. Asai Y, Makimura Y, Ogawa T (2007) Toll-like receptor 2-mediated dendritic cell activation by a Porphyromonas gingivalis synthetic lipopeptide. *J Med Microbiol* 56:459–465.
40. Makimura Y, et al. (2006) Correlation between chemical structure and biological activities of Porphyromonas gingivalis synthetic lipopeptide derivatives. *Clin Exp Immunol* 146:159–168.
41. Zhou Q, Amar S (2006) Identification of proteins differentially expressed in human monocytes exposed to Porphyromonas gingivalis and its purified components by high-throughput immunoblotting. *Infect Immun* 74:1204–1214.
42. Nguyen MT, et al. (2007) A subpopulation of macrophages infiltrates hypertrophic adipose tissue and is activated by free fatty acids via Toll-like receptors 2 and 4 and JNK-dependent pathways. *J Biol Chem* 282:35279–35292.